Available online at www.sciencedirect.com
SCIENCE DIRECT®
Journal of Nuclear Materials 344 (2005) 240–245
journal of nuclear materials
www.elsevier.com/locate/jnucmat

Characterization of fuel oxidation in rods with clad-holes

R.A. Verrall *, Z. He, J.F. Mouris

Chalk River Laboratories, Atomic Energy of Canada Limited, Chalk River, Ont., Canada K0J 1J0

Abstract

Three irradiated reactor rods that had holes in the cladding were examined for oxidation. The techniques used were coulometric titration and optical examination. Coulometric titration has the capability to measure the O/M ratio for small (~100 mg) samples. Both the longitudinal and radial directions of the rods were examined. Two of the rods had little oxidation. The third rod was oxidized everywhere, but especially at the clad-holes where the O/M values reached a maximum of 2.10. The difference between the three rods is examined. Qualitatively, optical examination revealed similar trends. For the third rod, oxidation proceeded more rapidly along the grain boundaries than within the grains themselves. Also, grain growth and gas bubble formation occurred, which had not been expected because the power levels were too low for that to occur. It seems that the temperatures were increased because of lower thermal conductivities in the higher oxide phases.

1. Introduction

Oxidation of UO_2 fuel pellets through holes in the clad affects important fuel properties: thermal conductivity and melting point; fission-product diffusion rates; uranium and oxygen diffusion rates; and enhanced grain growth and fission-gas release. These holes can allow water into the fuel, which can lead to oxidation. The objectives of this program were to develop techniques for reliable measurement of the O/M ratio as a function of radial and longitudinal pellet stack position and apply these techniques to fuels with cladding holes. The techniques used were coulometric titration (which will be described) and optical microscopy. Ultimately, the aim is to determine which are the main parameters that control the amount of fuel oxidation in fuel rods with clad-holes.

In the 1990s, Une [1] examined two defective Zircaloy-clad BWR fuel rods for oxidation, one that had been base irradiated, and one that had been power ramped. Oxidation was measured by lattice parameter measurements using X-ray diffraction along both the axial and diametral directions. Hyperstoichiometric UO_{2+x} was found, but no phase changes to higher-order oxides of U_4O_9 or U_3O_8 were located. The fuel oxidation depended significantly on the defect size and distance from the defect. The pellet volume-averaged O/M ratios at various axial locations were in the range of 2.02–2.06 for the base irradiated fuel, and about 2.01 for the power-ramped fuel. The relationship between fuel oxidation and secondary hydriding was also discussed. Une also referenced other authors who have reported on fuel oxidation at defects, but who didn't give quantitative information on the O/M stoichiometry along the axial and diametral directions as Une did. In those papers, the degree of fuel oxidation seems to depend on the

* Corresponding author. Tel.: +1 613 584 3311; fax: +1 613 584 3250.
E-mail address: verrallr@aecl.ca (R.A. Verrall).

0022-3115/$ - see front matter
doi:10.1016/j.jnucmat.2005.04.049

extent of deterioration of the fuel defects. In some cases, the Widmanstatten type structures of U_4O_9 needles were observed. In another, there was little departure from stoichiometry at the pellet centre, but which exhibited an increasing O/M ratio towards the pellet rim.

2. Measuring O/M ratio by coulometric titration

In a hot cell, 50–200 mg fuel samples were obtained from specific radial and longitudinal pellet stack locations in an irradiated fuel rod with a clad-hole. This was done by cutting ~10 mm pellet sections from the rod and drilling them at precise positions with a 1.8 mm diamond drill, parallel to the rod axis. Samples were then loaded into a glove box and placed in a furnace. This coulometric titration (CT) system works as follows (Fig. 1): With the furnace at room temperature, Ar gas containing 1300 ppm H_2 is passed over the sample. At room temperature, no reaction between the sample and gas occurs. Downstream the gas is passed through the ceramic CT cell which measures how much O/M-ratio (oxygen) is required to convert all the H_2 to H_2O (how this is done is described in the next paragraph). Next, the sample in the furnace is heated to 1000 °C, at (usually) 5 °C per minute. When the temperature becomes high enough, the gas and sample begin to react. The partial pressure of H_2 in the gas flow converts UO_{2+x} to stoichiometric UO_2. Since the temperature only rises to 1000 °C, the sample cannot become substoichiometric – that would take about 1500 °C or higher. This process continues until no further O is released from the sample, rendering it stoichiometric. The decrease in the amount of H_2 in the gas delivered to the CT cell is integrated, thereby allowing the amount of O being released from the sample to be calculated.

A schematic diagram of the ceramic CT cell is shown in Fig. 2. The gas flows down the centre of the tube. The wall of the tube is composed of zirconia (ZrO_2) doped

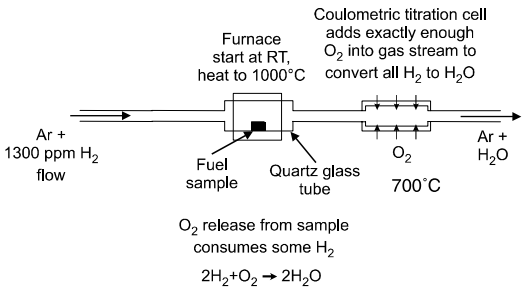

Fig. 1. Schematic diagram of coulometric titration apparatus. In an advanced mode, a second coulometric titration is placed in the flow stream upstream of the furnace to facilitate adding oxygen to the gas flow.

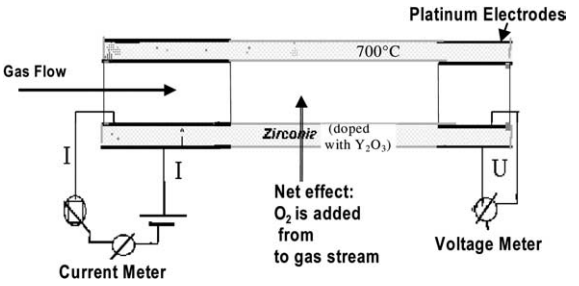

Fig. 2. Rough schematic diagram of a CT cell. Doping ZrO_2 with Y_2O_3 increases the O^{2-} vacancy concentration, thus enhancing its diffusion rate. Measuring the electric current (I) gives the O^{2-} diffusion rate. Measuring the voltage (U) gives the O_2 partial pressure inside the tube relative to the value outside the tube.

with 8 mol% yttria (Y_2O_3). During operation, the CT cell is always maintained at 700 °C. At this temperature, this material readily conducts O atoms (actually double-negative oxygen ions) through the lattice, but will not conduct free electrons as metals do. So, when an electrical voltage is applied, oxygen ions are free to move, but free electrons are not. Therefore, any electrical current measured is an indication of oxygen ion transport. At the gas inlet, a voltage is set up through the tube wall and current, in the form of oxygen ions, is allowed to flow. The air surrounding the tube allows O ions to form at the outer surface of the tube. They conduct through the wall where they recombine with other O ions at the inner surface and desorb from the cell surface as O_2 (or combine directly with the H_2 in the gas to form H_2O). In this way, O_2 is passed from the air atmosphere through the cell wall to the flowing gas stream interior to the CT tube. At the CT gas-outlet, the voltage between the inner surface and outer surface is measured. This voltage can be used to directly measure the O_2 partial pressure in the tube relative to the O_2 partial pressure in the air atmosphere. A feedback loop from this voltage is then set up to control the oxygen current inflow at the inlet end of the tube. In this way, only enough O_2 is provided to convert all the H_2 to H_2O. (Actually the O_2 content in the tube is always brought to a small fixed quantity of O_2 – about 40 ppm – that ensures that the H_2 quantity is extremely low.) One of the methods used to verify and calibrate the CT equipment is the following: we prefabricate U_3O_8 and then measure the change in stoichiometry to bring it to UO_2. We require the error in these tests to be below 1% of the change in O/U ratio. For UO_2 samples with lower O/U ratios – about 2.10 – uncertainty is about 5% of the change in stoichiometry (i.e., 0.005). Another source of uncertainty is the following: when the sample is finely ground, which occurs for dense non-friable samples of irradiated UO_2, a slight amount of oxidation of powder occurs between drilling and measurement. This can lead to an uncertainty of

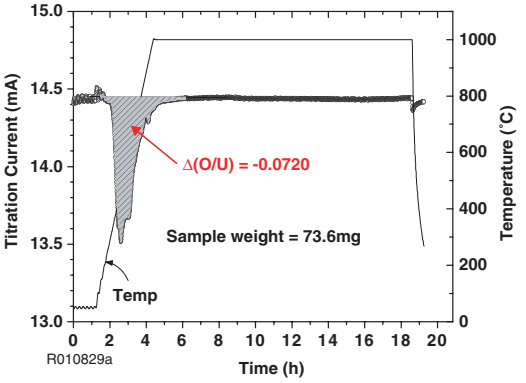

Fig. 3. Reduction of an irradiated sample of fuel with a clad-hole.

0.01 in the change in stoichiometry. For dense non-friable samples, this is the major source of error.

Fig. 3 shows the results of an O/M-ratio measurement of an actual irradiated fuel sample from a rod with a cladding hole. The *titration current* in this figure represents the amount of O ions needed in the CT cell to exactly convert all the H_2 to H_2O. Assuming that all the oxygen released from the sample during the measurement came from altering the stoichiometry of the UO_2, and not from other phases that may have been present, the fuel sample had an initial stoichiometry of $UO_{2.072}$ in this example. However, this is an upper limit because other phases in the fuel sample, for example higher uranium oxide phases and/or fission-product phases, might also have released oxygen.

3. Advanced mode of CT operation

Putting a second CT cell in the gas flow *upstream* of the sample furnace increases the usefulness of the equipment. This upstream cell can add oxygen to the gas flow and thus provide for the creation of oxidized samples in the heating furnace. For example, as a function of O_2 content in the gas, unpublished O/M measurements of $(U, Dy)O_2$ fuel shows that it is more resistant to stoichiometry changes than UO_2. (The presence of Dy in $(U, Dy)O_2$ is a possible choice of a burnable poison in CANDU® reactors to control reactivity and to increase burnup.) Both the kinetics and the total amount of absorbed oxygen can be compared for these two materials.

4. Fuel rods with clad-defects

All the analysed rods had been discharged for more than 5 years. Table 1 gives information on the burnup and clad-hole sizes. Rod C was recovered within 1 day after hole formation. Rods A and B were irradiated longer than 10 days after hole formation. Besides primary defects (e.g., debris fretting), each rod also had secondary defects, caused by hydride cracking along the interior of the tube wall [2–5].

5. Results

5.1. O/M observations measured by CT

Only Rod A showed clear signs of pellet oxidation (Fig. 4). For this rod, all samples showed oxidation (i.e., the centre section as well as the end sections, and the interior as well as the exterior samples). The centre cross-section showed slightly lower O/M values than the end-sections because the clad-holes had occurred at both end positions. The O/M values ranged from 2.02 to 2.10. Rods B and C typically showed O/M values close to 2.00. Only a few values at secondary defects showed O/M values of 2.01 to 2.02.

5.2. Optical microscopy for Rod A

In agreement with oxidation measurement by CT, optical microscopy of Rods B and C did not reveal any signs of UO_2 oxidation. Moreover, the grain sizes were typical for intact fuels irradiated under similar operating conditions. Only Rod A indicated the presence of higher oxide phases and enhanced grain growth. Microscopy of Rod A follows.

5.2.1. Primary defect

The primary defect (i.e., fretting defect) in Rod A was small and no UO_2 loss was observed. However, UO_2

Table 1
Summary of operating conditions and clad-holes

Rod	Peak linear power (kW/m)	Burnup (MWd/kgU)	Failure root cause	PDRT[a] (days)	Defect size area (mm^2)
A	29	3.4	Debris fretting	>10	~13
B	35	3.5	Incomplete closure weld	>10	⩽1.5
C	50	7.3	SCC[b]	<1	<1

[a] Post-defect residence time (">10" is an estimate based on internal sheath oxidation).
[b] Stress–corrosion cracking.

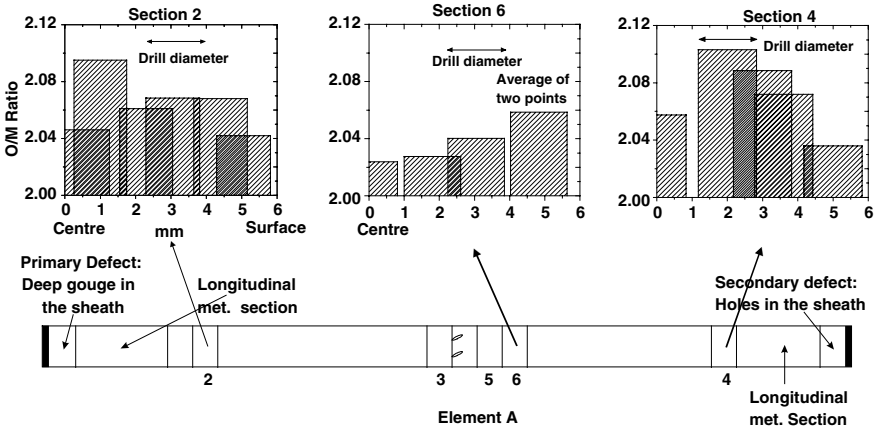

Fig. 4. O/M measurements for element A.

oxidation was observed along the exterior of the pellet and at a major radial crack (Fig. 5). Also, the grain boundaries in this vicinity were oxidized (Fig. 6). Moreover, at the centre in this region, the grain size was about 17 μm compared with 6 μm at the periphery (as-manufactured grain size was 6 μm). This, and the observation that many intergranular gas bubbles and tunnels were observed, are features not expected at this power (29 kW/m) and burnup (3.4 MWd/kgU) for intact rods. Rather, they support the observations of pellet oxidation in this region, since pellet oxidation can reduce thermal conductivity, thereby enhancing UO_2 grain growth and fission-gas release [6].

5.2.2. Secondary defect

The secondary defect of Rod A was relatively large (about 13 mm^2) and UO_2 loss near the defect was apparent (see Fig. 7). There were two regimes analysed in this region: (a) the defect itself, and (b) the pellet-to-pellet interface nearby the defect, shown in Fig. 7.

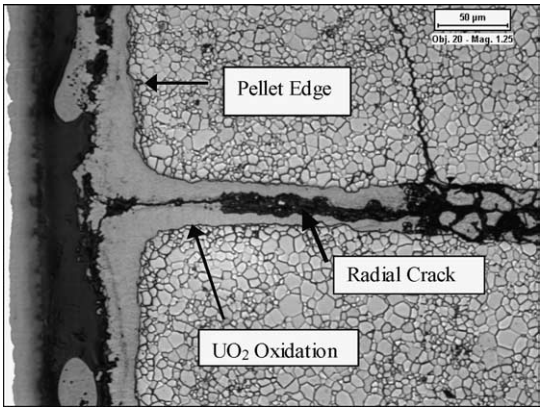

Fig. 5. Primary (fretting) clad-hole – shows fuel oxidation on the pellet edge and radial crack.

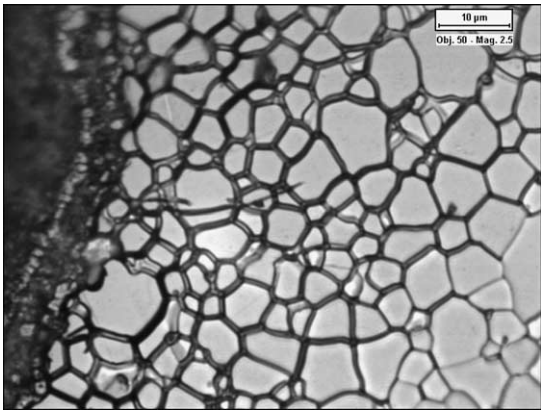

Fig. 6. Primary (fretting) clad-hole – higher magnification than Fig. 5, showing fuel grain boundary oxidation near a radial crack.

5.2.2.1. At the secondary defect. Loss of fuel and loose grains were observed. In the mid-radius of this region, fuel oxidation was observed at cracks (Fig. 8). Islands of grains appeared throughout the oxidation phase, indicating preferential grain boundary oxidation. In the central region (not shown), oxidation along radial cracks was also observed, but the extent of oxidation was not as great as that in the mid-radius region.

Besides oxidation, UO_2 grain growth was observed in both the mid-radius (14 μm), shown in Fig. 9, and the central regions (30 μm) – versus 6 μm as-fabricated. Also gas bubbles and tunnels were observed at the grain boundaries in both regions. These are all evidences of decreased thermal conductivities.

Fig. 7. At secondary hole, low magnification – shows fuel loss from hole, cracks, and a pellet-to-pellet interface (at arrow).

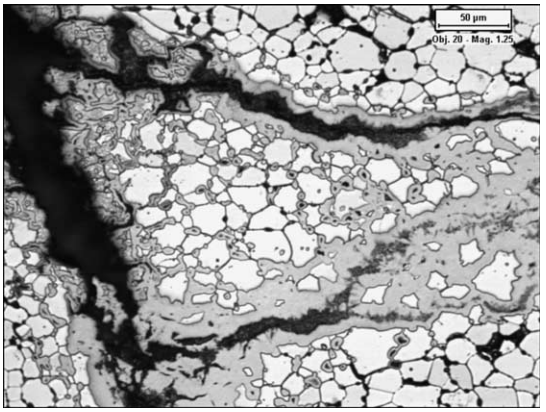

Fig. 8. At secondary hole mid-radius (i.e., 3.5 mm from the centre) along a radial crack – shows isolated grains embedded in darker fuel oxidation.

5.2.2.2. Pellet-to-pellet interface. Shown in Figs. 7 and 10, UO_2 oxidation was greatest at about 3 mm from the pellet centre line, where it was 350 μm thick (in comparison, the radius of rod is 6 mm). Radial and axial cracks were seen. At 2 mm from the centre line (Fig. 11), the oxidized layer at the interface was thinner (80–130 μm). Also, islands of isolated UO_2 grains embedded in the oxidized grey areas were seen. Moreover, as seen elsewhere, UO_2 oxidation took place more quickly along the grain boundaries than within the grain. Near the centre line, the oxide thickness at the interface was about 110 μm and exhibited columnar grain growth (Fig. 12).

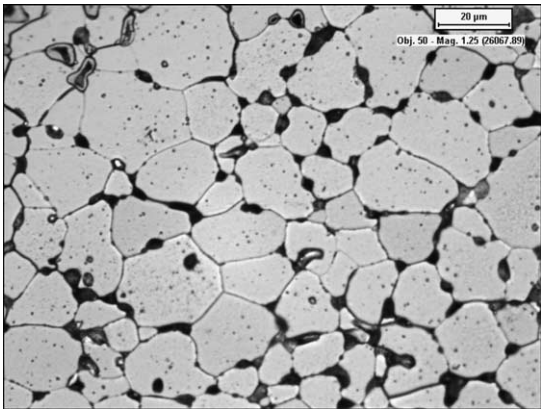

Fig. 9. At secondary hole mid-radius (i.e., 3 mm from centre) – shows grain growth (average grain size 14 μm), and fission-gas bubbles in grain boundaries and tunnels.

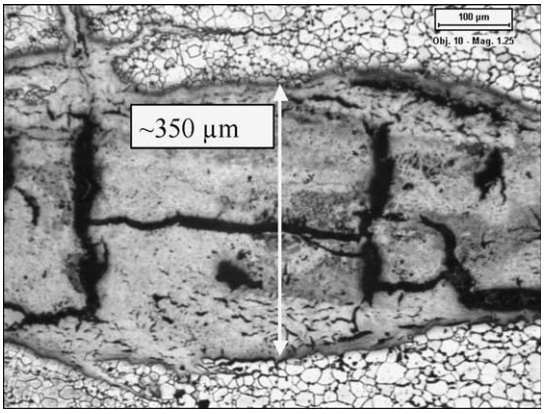

Fig. 10. Pellet-to-pellet interface near secondary hole, 3 mm from centre line – shows the thickness of the oxidized layer was about 350 μm.

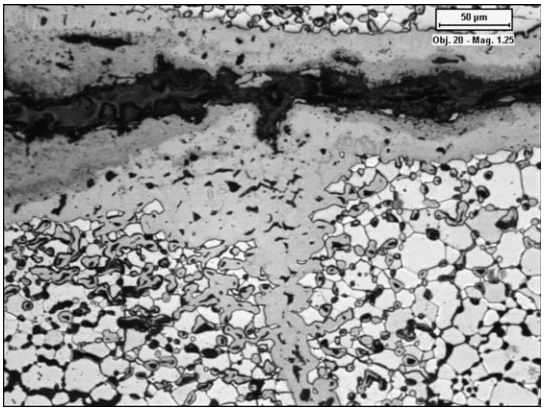

Fig. 11. Pellet-to-pellet interface near secondary hole, 2 mm from pellet centre line – shows general oxidation along centre line, and islands of normal fuel grains.

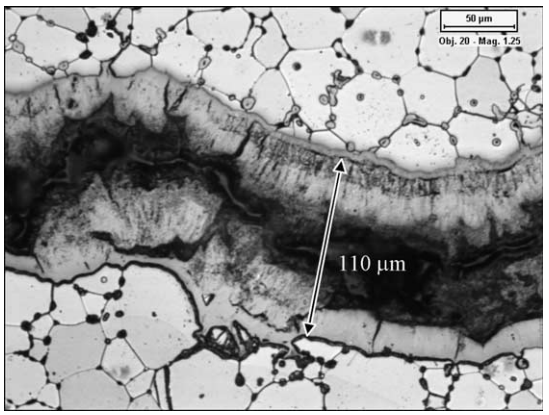

Fig. 12. Pellet-to-pellet interface near secondary hole, at centre line – shows grain growth (30 mm) with gas bubbles and tunnels along the grain boundaries. Also shows fuel oxidation with columnar grain growth at the interface. The thickness of the oxidized layer was about 110 μm, as shown.

6. Conclusions

In three irradiated fuel rods with clad-holes, O/M measurements based on coulometric titration and optical microscopy produced converging results. Two of the rods did not show much oxidation, but one showed O/M ratios between 2.02 and 2.10. Also, the agreement between the two techniques occurred as a function of position within the rods themselves, at least qualitatively.

The rest of the conclusions are specific to Rod A:

(a) At the secondary defect, Rod A was more oxidized, radially, at the mid-radius than at the centre or surface regions. It is not completely clear if this also occurs at the primary defect, but it is not true at the longitudinal centre of the rod. The reason for the difference is not known.
(b) Oxidation proceeded more rapidly along the grain boundaries than within the grains themselves, allowing, for example, islands of grains appearing within the oxidation.
(c) At the defects themselves, grain growth and gas-bubble formation occurred, a feature that would not have been expected in intact rods. This suggests that the oxidation decreased the thermal conductivity allowing both diffusion rates to occur more rapidly.

Since thermodynamics at the reactor-operating temperatures, especially at the centre, suggests that phase changes wouldn't occur, we are experimenting now to see if these phase changes were caused during element cooling after discharge. The overall degree of oxidation isn't in question, because the grain growth and fission-gas bubble require in-reactor temperatures to occur. The only question is whether the changes in phase occurred in-reactor or out-reactor.

References

[1] K. Une, M. Imamura, M. Amaya, Y. Korei, J. Nucl. Mater. 223 (1995) 40.
[2] J.M. Markowitz, WAPD-TM-351, Bettis Atomic Power Laboratory, 1963.
[3] D.H. Locke, Nucl. Eng. Des. 21 (1972) 318.
[4] D.R. Olander, W. Wand, Y.S. Kim, C. Li, K. Lim, J. Nucl. Mater. 248 (1997) 214.
[5] B.J. Lewis, R.D. MacDonald, N.V. Ivanoft, F.C. Iglesias, Nucl. Technol. 103 (1993) 220.
[6] B.J. Lewis, J. Nucl. Mater. 160 (1988) 209.